(This is a sample cover image for this issue. The actual cover is not yet available at this time.)

Synthetic Metals 167 (2013) 64–71

Contents lists available at SciVerse ScienceDirect

Synthetic Metals

journal homepage: www.elsevier.com/locate/synmet

Electrical and electrochemical properties of polystyrene/polyaniline core–shell materials prepared with the use of a reactive surfactant as the polyaniline shell precursor

Alejandro Vega-Rios [a], Claudia A. Hernández-Escobar [a], E. Armando Zaragoza-Contreras [a,*], Takaomi Kobayashi [b]

[a] Centro de Investigación en Materiales Avanzados, S.C. Miguel de Cervantes No. 120, Complejo Industrial Chihuahua, Chihuahua, Chih., Mexico
[b] Department of Materials Science and Technology, Nagaoka University of Technology, 1603-1 Kamitomioka, Nagaoka, Japan

ARTICLE INFO

Article history:
Received 30 October 2012
Received in revised form 12 February 2013
Accepted 13 February 2013

Keywords:
Conducting polymer
Core–shell composite
Inverse surfmer
Polyaniline
Surfmer

ABSTRACT

Series of polystyrene/polyaniline core–shell composites were synthesized by adding reactive surfactant anilinium dodecylsulfate (DS-AN) as the monomer of polyaniline. DS-AN conversion to polyaniline was calculated by quantitative infrared spectroscopy and thermogravimetric analysis, showing both methods small differences. Composites particle size distribution showed no clear evidence of increment in the overall composite particle diameter as function of polyaniline content; however, electron microscopy (HR mode) showed that the conductive polymer was deposited over the polystyrene cores in the form of thin coatings. Composites electrical conductivity, determined by the 4-probe technique, was in the range 10^{-6} to 10^{-2} S cm^{-1}. The percolation–tunneling mechanism, according to the curve of conductivity (S cm^{-1}) versus polyaniline (wt%), was the electron transfer mechanism. Finally, all the composites were electroactive, as shown by cyclic voltammetry.

1. Introduction

Conducting polyaniline (emeraldine base salt) has been commonly mixed with thermoplastic polymers to overcome processability limitations of polyaniline (PAni) derived of its infusibility and poor solubility in common solvents. PAni/thermoplastic composites are quite popular because depending on the thermoplastic matrix conducting composites with different attributes can be obtained [1–5]. Colloidal PAni/thermoplastic core–shell composites are a particular form to produce conducting composites. This kind of arrangement allows controlling composite morphology and composition. Among the wide variety of combinations with thermoplastics, the polystyrene/polyaniline core–shell composites have been widely reported. In these studies, the strategy to deposit the shell of polyaniline has been greatly varied. For instance, Barthet et al. [6] synthesized PAni-coated polystyrene latexes. Nonuniform PAni coatings were obtained using conventional aniline polymerization conditions (aniline monomer, ammonium persulfate, 1.2 M HCl at 25 °C). In contrast, more homogeneous PAni coatings were obtained when polymerizing aniline hydrochloride at 0 °C in water. Yang and Liau [7] developed a methodology for fabricating nanostructured PAni films from polystyrene/PAni core–shell particles. Results showed that due to their large surface area and porosity, the films response was fast to different conditions, especially to dry gas flow and ethanol vapor. Wang et al. [8,9] obtained polystyrene particles coated with PAni by the "Swelling diffusion interfacial-polymerization method". This method allowed them to control morphology and uniformity of the PAni overlayer. Dai et al. [10] obtained hollow carbon spheres by using as templates polystyrene/polyaniline core–shell composites. In this methodology, the polystyrene particles were first sulfonated and then surface functionalized by aniline. Afterwards, the aniline salt was polymerized by adding the oxidizing agent, in this case, ammonium persulfate. The last step was the carbonization of the organic material.

In this study, we have used anilinium dodecylsulfate (DS-AN) as a precursor of conducting polyaniline to synthesize series of polystyrene/polyaniline core–shell composites. In particular, the characterization of electroconducting and electroactive properties was of great interest, as an intermediate step toward potential and practical applications; i.e., in chemical sensor design. DS-AN represents as a new concept of reactive surfactant or surfmer, as its functionality lies on the anilinium group and not on the polymerizable carbon–carbon double bond. This feature greatly distinguishes DS-AN from the traditional surfmer concept [11–14]. However, the intention is similar that DS-AN performs as a

* Corresponding author. Tel.: +52 614 439 4811; fax: +52 614 439 1130.
E-mail address: armando.zaragoza@cimav.edu.mx (E.A. Zaragoza-Contreras).

0379-6779/$ – see front matter © 2013 Elsevier B.V. All rights reserved.
http://dx.doi.org/10.1016/j.synthmet.2013.02.009

Table 1
Formulations of the core–shell composites.

[a]Formulation	Core (g)	[b]DS-AN (g)	[c]APS (g)
DS-AN 6	3.6	0	0.1756
DS-AN 10	3.6	0.1695	0.3048
DS-AN 15	3.6	0.4048	0.4842
DS-AN 20	3.6	0.6695	0.6857
DS-AN 30	3.6	1.3123	1.1760
DS-AN 40	3.6	2.1695	1.8290

[a] Numerical value indicates weight percent of DS-AN used in the synthesis of the shell. That is, in DS-AN 6, 6 wt% of DS-AN was used.
[b] DS-AN (g) added considering the content of it in the latex (0.2305 g).
[c] In all experiments the molar ratio DS-AN:APS was 1.0:1.2.

surfactant and as a monomer of polyaniline. Previously, we reported the characterization, critical micellar concentration (cmc), and applied DS-AN as the surfactant in the synthesis of polystyrene via emulsion polymerization, making clear DS-AN properties as a surfactant [15].

It is worth saying that conventional polymerizable surfactants (surfmers) are a special family of surfactants. Their composition includes a hydrophilic group (ionic or non-ionic), a hydrophobic hydrocarbon chain, and a free radical polymerizable carbon–carbon double bound linked to the hydrocarbon chain. These compounds are especially attractive because, besides acting as conventional emulsifiers, they can be covalently linked to a latex particle surface [16,17]. Numerous reports have described state-of-the art over the years [18–21]; for this reason, their various aspects will not be detailed here.

It is also important to comment that the concept of polymerizable anilinium salts is not new. Literature indicates that anilinium salts derived mainly from dodecylbencensufonate or dodecylsulfate have been reported. Sometimes the salts have been isolated and polymerized to polyaniline [22–24] and some others were formed in situ during PAni polymerization as reported by several authors [25–28]. However, to the best of our knowledge the double function surfactant/monomer for the anilinium salts has not been proposed before.

2. Experimental

2.1. Materials

Sodium dodecylsulfate (Aldrich Co.), ammonium persulfate (Aldrich Co.) and hydrochloric acid (J.T. Baker) were used as received. Aniline and styrene monomer (Sigma–Aldrich) were distilled under vacuum. 2,2′-azobis(2-methylpropionamidine) dihydrochloride (Aldrich co.) was recrystallized from a saturated aqueous solution at 60 °C. The solvents 1,4 dioxane (99%), *N*,*N*′-dimethylformamide (DMF, >99%) and ammonium hydroxide were used as received and bought from Sigma–Aldrich.

2.2. Core–shell composites

The synthesis of the polystyrene/polyaniline core–shell composites has been reported previously [15]. On the one hand, polystyrene core was synthesized by conventional emulsion polymerization using DS-AN (20 mmol dm^{-3}) as the stabilizer, and 2,2′-azobis(2-methylpropionamidine) dihydrochloride (0.00184 mol dm^{-3}) to launch free radical polymerization. On the other hand, polyaniline shell was obtained via oxidative polymerization. In this stage, extra amount of DS-AN was added as the monomer of polyaniline. Ammonium persulfate (APS) was used as the oxidizing agent at a molar ratio of 1.2:1.0 (DS-AN:APS). Details of the different formulation are given in Table 1.

2.3. Characterization

2.3.1. Electron microscopy

Scanning electron microscopy in transmission mode (STEM) was performed in a field emission electron microscope (JSM-7401F; JEOL) at 30 kV. To prepare the samples, two drops of latex were dispersed using sonication for 5 min in 30 mL of tridistilled water. Subsequently, a drop of latex was placed and left dry on a holey-carbon-cooper grid. By this procedure, the latexes, the core–shell composites, and the samples of pure PAni were analyzed.

2.3.2. UV–vis spectroscopy

Absorption spectra of polystyrene/polyaniline composites were acquired using a UV–vis spectrometer (Lambda 10, Perkin Elmer). Samples were prepared by dedoping of polyaniline shell with ammonium hydroxide, and then, solving the products in a mixture of DMF:1,4 dioxane (80:20).

2.3.3. Infrared spectroscopy (FTIR)

FTIR spectra were recorded by using a Fourier transform spectrometer (Spectrum GX, Perkin Elmer) using attenuated total reflection (ATR) technique at room temperature. Quantitative analysis was performed by establishing a calibration curve (see supplementary material Fig. S1). Polystyrene/PAni blends with compositions in the range of 6–30 wt% PAni were prepared by solution mixing. The band at 1492 cm^{-1}, present in both polymers but not in dodecylsulphate anion, was taken to determine PAni content.

2.3.4. Electrical conductivity

Electrical conductivity was determined by the 4-point technique using a homemade device. Pellets of each core–shell composite and pure PAni (2 mm width × 13 mm diameter) were prepared by compression at laboratory conditions. A conductivity meter (34410A 6 1/2 Digit, Agilent) was used to determine resistivity.

2.3.5. Cyclic voltammetry

The core–shell composites were characterized by cyclic voltammetry (CV) using a potentiostate analyzer (model 1260 plus 1287, Solartron). The software CorrView 2 was used to visualize the graphics. Electrochemical measurements were performed in a standard three-electrode cell at room temperature, using Pt wire (area = 0.03 cm^2) as the counter electrode, and Ag/AgCl/saturated KCl as the reference electrode. The working electrode was a Teflon cylinder packed with carbon paste, with a copper wire inserted through one end of the cylinder. The sample of dried composite was deposited on the opposite end to copper wire. The electrolyte was a sulfuric acid (H_2SO_4) solution 0.1 mol dm^{-3}. All cyclic voltammogram were recorded at a scan rate of 50 mV s^{-1} by sweeping the potential between −800 and +1400 mV against Ag/AgCl reference electrode.

2.3.6. Composite composition

Composites composition was characterized using a thermogravimetric analyzer (SDT Q600, TA Instruments). The evaluations were performed under air atmosphere at a heating rate of 10 °C min^{-1}.

3. Results and discussion

3.1. Core–shell composites synthesis and morphology

In this work, emulsion polymerizations stabilized with DS-AN were used to produce the polystyrene core of the composites. The kinetics of the different polymerized systems was previously reported [15]. The second stage of the composite synthesis was performed via an oxidative polymerization. Therefore, more DS-AN

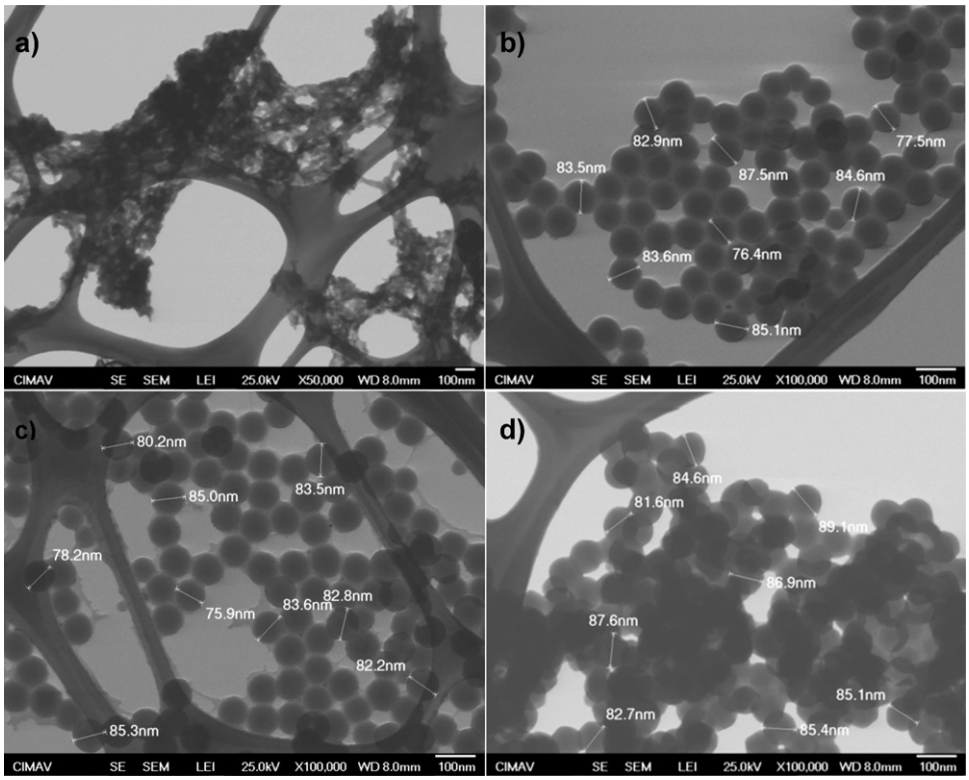

Fig. 1. Micrographs of TEM. (a) PAni, (b) polystyrene, (c) polystyrene/PAni 6 wt% DS-AN, and (d) polystyrene/PAni 40 wt% DS-AN.

was added as the monomer of PAni. Series of composites corresponding to proportions of 6, 10, 15, 20, 30, or 40 wt% DS-AN, with respect to polystyrene content, were synthesized. The final products of this stage were green-stable dispersions. Fig. 1(a)–(d) portraits micrographs of pure polyaniline, pure polystyrene, and core–shell composites synthesized with 6 and 40 wt% DS-AN.

Pictures with the lowest and the highest concentrations of DS-AN were only included since no visual differences among the composites were observed. The polyaniline (PAni) obtained from DS-AN is usually observed in the form of large agglomerations of semispherical and elongated particles with variable dimensions. The polystyrene particles, on the other hand, are well defined spherical particles with diameters in the range of 80 nm and evident narrow polydispersity. Concerning the core–shell composites, no appreciable change in the particle size, with respect to the control of polystyrene or among themselves, was observed. A modest progressive surface deformation with the increment of DS-AN was only observed. Furthermore, the presence of a separate phase of PAni was not observed in any of the composites, which suggested that most of the polyaniline was deposited on the polystyrene cores.

Fig. 2 shows the curves of particles size distribution of all the composites. In accordance with microscopy observations, all the distribution curves were similar, with average particle size in the range of 80 nm, independently on the content of DS-AN. These results suggested that composites' shells thickness were very thin, apparently not more than 5 nm. This finding is contrasting with literature since reports on core–shell composites with shells of polyaniline, usually exhibit clear depositions of the conducting polymer, where commonly the shell is constituted by PAni aggregates [29–32]. Even though, some other groups have developed tactics to produce composites with uniform and controllable polyaniline shells [9]. From these initial results, the formation of the PAni shells on the composites was truly uncertain, even though, as mentioned above, the formation of a separate phase of PAni was not observed in any composite.

3.2. UV–vis spectroscopy

UV–vis absorption spectra of polystyrene/PAni composites are show in Fig. 3. As observed, band intensity is more prominent for the formulations with higher DS-AN content. Two bands, one at 620 nm (2 eV) and another at 329 nm (3.8 eV) due to the π–π^* transition of the benzenoid rings (—B—NH—B—NH—), and π–π^* transition of the quinoid rings (—B—N=Q=N—) segments, respectively, typically present in PAni, are observed. Bands' absorption indicated that DS-AN was polymerized to PAni, that spectrum intensity indicated a progressive increment of PAni content as DS-AN incremented in the formulation, and that the PAni is in the form of emeraldine base salt as reported in literature [33,34].

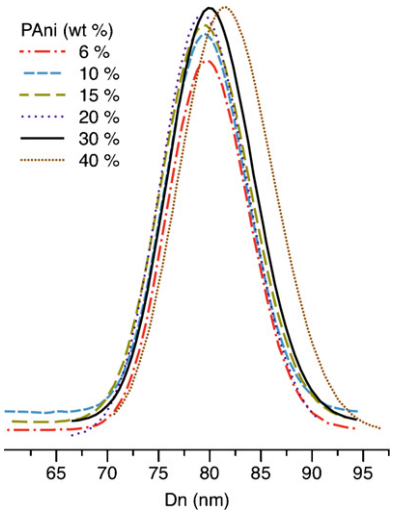

Fig. 2. Particles size distribution of the polystyrene/PAni core–shell composites.

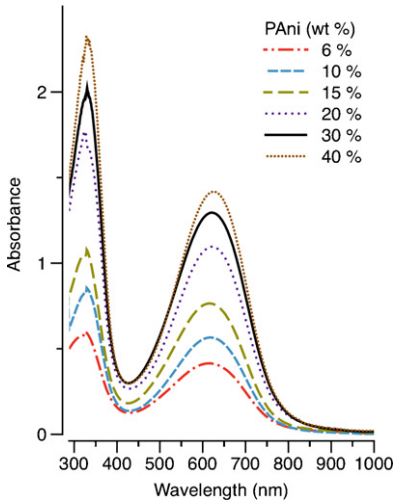

Fig. 3. UV–vis absorption spectra of polystyrene/PAni composites. Samples were prepared by dedoping of polyaniline shell with ammonium hydroxide, and then, solving the products in a mixture of DMF:1,4 dioxane (80:20). (For interpretation of the references to color in figure legend, the reader is referred to the web version of the article.)

3.3. Infrared spectroscopy

Even though microscopy has not given clear evidence of PAni shells, UV–vis spectroscopy showed, based on the spectrum intensity, that polyaniline content was higher for the formulations with higher DS-AN content. To characterize composite composition, quantitative infrared analysis (by ATR mode) was performed. All composites spectra showed a combination of polystyrene and polyaniline patterns. Furthermore, progressive evolutions of several peaks, some of them increasing and some others reducing, are observed (see supplementary material Fig. S2). Of course, these changes are not attributed to chemical reactions, but to mass effects; that is, because of the polystyrene:polyaniline weight content in the composite.

As infrared spectroscopy of polystyrene/PAni composites has been widely reported in literature, this aspect will not be treated in detail here [35,36], and we will concentrate in the peaks that can be correlated with the polymer:polymer weight fraction. The characteristic peaks of PAni appear at 1492 and 1583 cm^{-1}, as observed in Fig. 4. These bands are ascribed to the stretching vibration of benzenoid and quinoid rings ($[(-B-NH-B-NH-)_y(-B-N=Q=N-)_{1-y}]_x$, where B and Q denote, respectively, C_6H_4 rings in the benzenoid and quinoid forms) [37–39]. The bands at 1240, 1300, and 1369 cm^{-1} is related to the stretching vibrations of charged nitrogen segments, and provides information about the charge delocalization in the PAni chains [40].

The peak at 1240 cm^{-1} is interpreted as a $C-N^+$ stretching vibration in the polaron structure, where the characteristic band of the conducting protonated form is located [41,42]. The band at 1300 cm^{-1} corresponds to π-electron delocalization induced in the polymer by protonation. In addition, the band at 1369 cm^{-1} is assigned to the weak C—N stretching absorption in QBQ units.

Infrared spectroscopy in quantitative mode was achieved with the aid of the calibration curve obtained with blends of polystyrene/PAni. Height variation of the peak at 1492 cm^{-1} was selected to determine quantitative values based on the correlation of PAni content both in the blends and in the core–shell composites, as shown in Table 2. It is worth saying that the other pointed bands may also be used for quantitative analysis determination (For example, the calibration curve considering the band at 1600 cm^{-1}, Fig. S1, and PAni compositions with reference to this peak, Table S1, are shown in the supplementary material). As observed, PAni content in the composites was lower than the content of DS-AN added for shell synthesis; that is, not all DS-AN was converted to PAni.

Most conversions were around 80%, which may be considered good yield. In the case of the lowest DS-AN content, conversion was slightly above 50%. In this case, no more DS-AN was added, only the DS-AN used during core synthesis was subjected to oxidative polymerization. Apparently, the surfmer was strongly adhered on the polystyrene particles surface, presenting limited mobility and, consequently, only a fraction, in the range of 50%, participated in the synthesis of PAni.

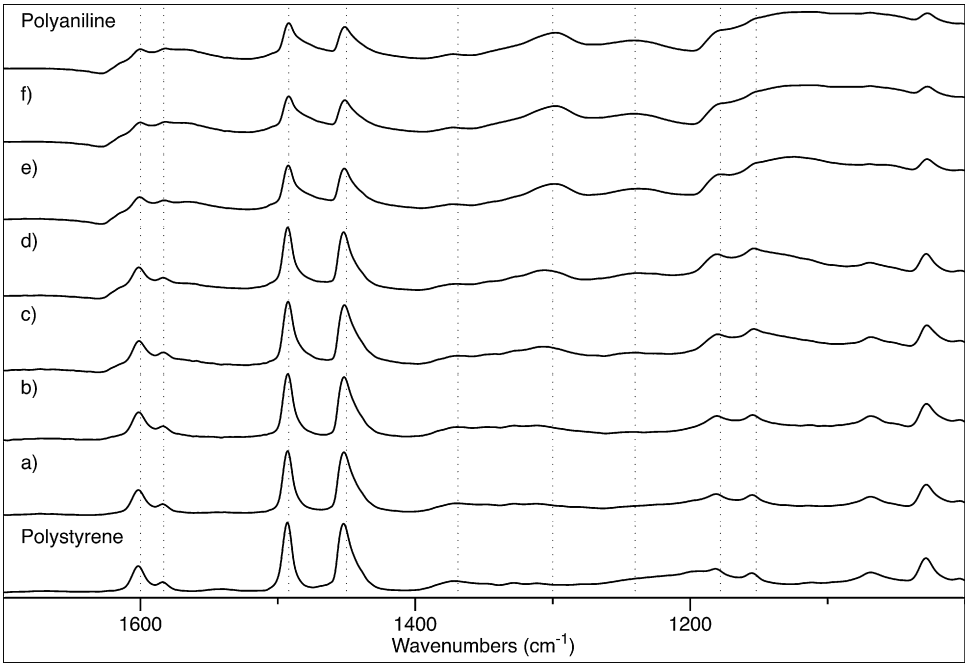

Fig. 4. FTIR spectra of PAni, polysterene, and polystyrene/PAni composites. (a) 6, (b) 10, (c) 15, (d) 20, (e) 30, and (f) 40 wt% DS-AN.

Table 2
PAni content in the core–shell composites based on the calibration curve.

Blend	PAni (wt%)	Height (mm)	Core–shell	Height (mm)	PAni (wt%)	PAni (%)
I	6.5	0.2224	DS-AN 6	0.2101	3.4	56.6
II	9.7	0.2278	DS-AN 10	0.2263	8.8	88.0
III	13.0	0.2362	DS-AN 15	0.2372	12.5	83.3
IV	17.0	0.2510	DS-AN 20	0.2459	15.4	77.0
V	23.4	0.2691	DS-AN 30	0.2700	23.5	78.3
VI	29.9	0.2902	DS-AN 40	0.2967	32.5	81.2

Note. Both height values for the polystyrene/PAni blends and for the core–shell composites correspond to an average of 3 different FTIR spectra.

3.4. Thermogravimetric analysis

As a complementary technique to characterize core–shell microstructure and composition, thermogravimetric analysis (TGA) was performed. The traces of polystyrene core, pure polyaniline obtained with DS-AN via oxidative polymerization, and the different core–shell composites are shown in Fig. 5. As observed, the core–shell composites presented clear combination of pristine polymers profiles, with more similarity to polystyrene at lower concentrations, and to PAni at higher concentrations. In particular, the transition observed at ca. 350 °C, associated to PAni backbone degradation [43], is perfectly observed in all the composites (ca. 450 °C), and is associated to the proportion of PAni in the composite. By considering this transition, it was possible to determine DS-AN conversion to PAni. In this manner, the weight fraction in the range of 350–800 °C, which corresponded to ca. 75 wt% of the total sample of the pure PAni, was considered as a sample of PAni at 100% conversion. Then, for instance, the composite of formulation DS-AN 15 (15 wt% DS-AN) indicated content of ca. 10 wt% of PAni (450–550 °C). Simple mathematical calculations indicated ca. 89% conversion of DS-AN to PAni; that is, PAni content was about 13.3 wt% in the composite. The calculated conversions of PAni are reported in Table 3. In this case, most conversions were in the range of 90%, excepting the formulation with 6 wt% DS-AN. By comparing DS-AN conversion to PAni by FTIR and TGA, we observe that some of the values matched very well, and some others presented slight deviation. It was considered that such deviations might be related to weighing precision. From these results, we consider that both techniques are suitable to determine conversion, even though the small observed differences. In advance, results are discussed based on the content of PAni determined by thermogravimetry, using the nomenclature suggested in Table 3.

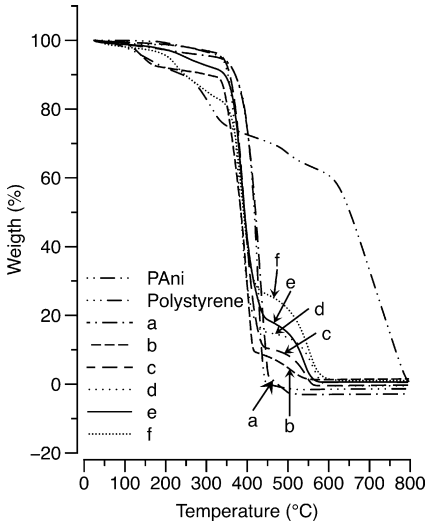

Fig. 5. TGA traces of PANi, polystyrene, and polystyrene/PAni composites. (a) 6, (b) 10, (c) 15, (d) 20, (e) 30, and (f) 40 wt% DS-AN. The evaluations were performed under air atmosphere at a heating rate of 10 °C min^{-1}.

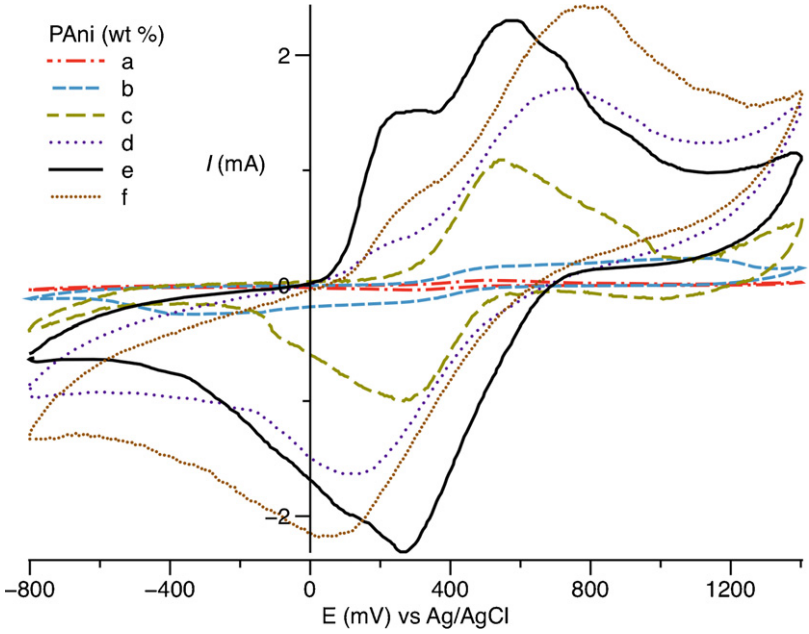

Fig. 6. Voltammograms of polystyrene/PAni composites. (a) CPAni 3.3, (b) CPAni 8.0, (c) CPAni 13.3, (d) CPAni 18.7, (e) CPAni 26.7, and (f) CPAni 37.3. A Pt wire and a Ag/AgCl/saturated KCl electrode were used, respectively, as the counter electrode and the reference electrode. The electrolyte was a H_2SO_4 solution 0.1 mol dm^{-3}.

Table 3
Conversion of DS-AN to PAni determined by TGA.

Composite	DS-AN comp. (wt%)	[a]PAni TGA (wt%)	[b]PAni comp. (wt%)	[c]Conversion (%)
CPAni 3.3	6	2.5	3.3	55.6
CPAni 8.0	10	6	8.0	80.0
CPAni 13.3	15	10	13.3	88.9
CPAni 18.7	20	14	18.7	93.3
CPAni 26.7	30	20	26.7	88.9
CPAni 37.3	40	28	37.3	93.3

[a] wt% PAni determined by TGA.
[b] wt% PAni in the composite calculated by: wt% PAni TGA × 100/75.
[c] Conversion (%) of DS-AN to PAni calculate by: (DS-AN in the formulation (g)/PAni composite wt (%)) × 100.

Table 4
The oxidation and reduction potentials of core–shell composites.

[a]Composite	[b]E_{pc} (mV)	[c]E_{pc} (mV)	E_{pa} (mV)
CPAni 3.3	–	498	284
CPAni 8.0	568	1122	356
CPAni 13.3	–	550	266
CPAni 18.7	260	741	124
CPAni 26.7	272	576	265
CPAni 37.3	283	777	64

[a] The numerical value indicates the content of PAni in the composite determined by thermogravimetry.
[b,c]Indicate, respectively, the first and the second peak in the voltammograms reported in Fig. 6.

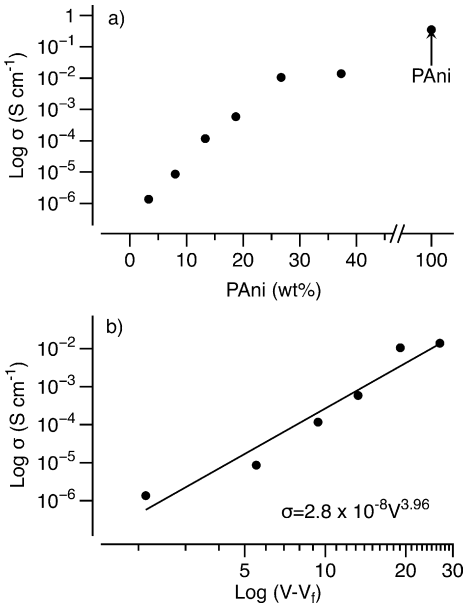

Fig. 7. (a) Electrical conductivity (σ) of the polystyrene/PAni composites as function of PAni content. Logarithmic plot of conductivity (σ) versus ($V - V_f$). The solid line is a fit to the percolation scaling law giving $V_f = 0.042\%$.

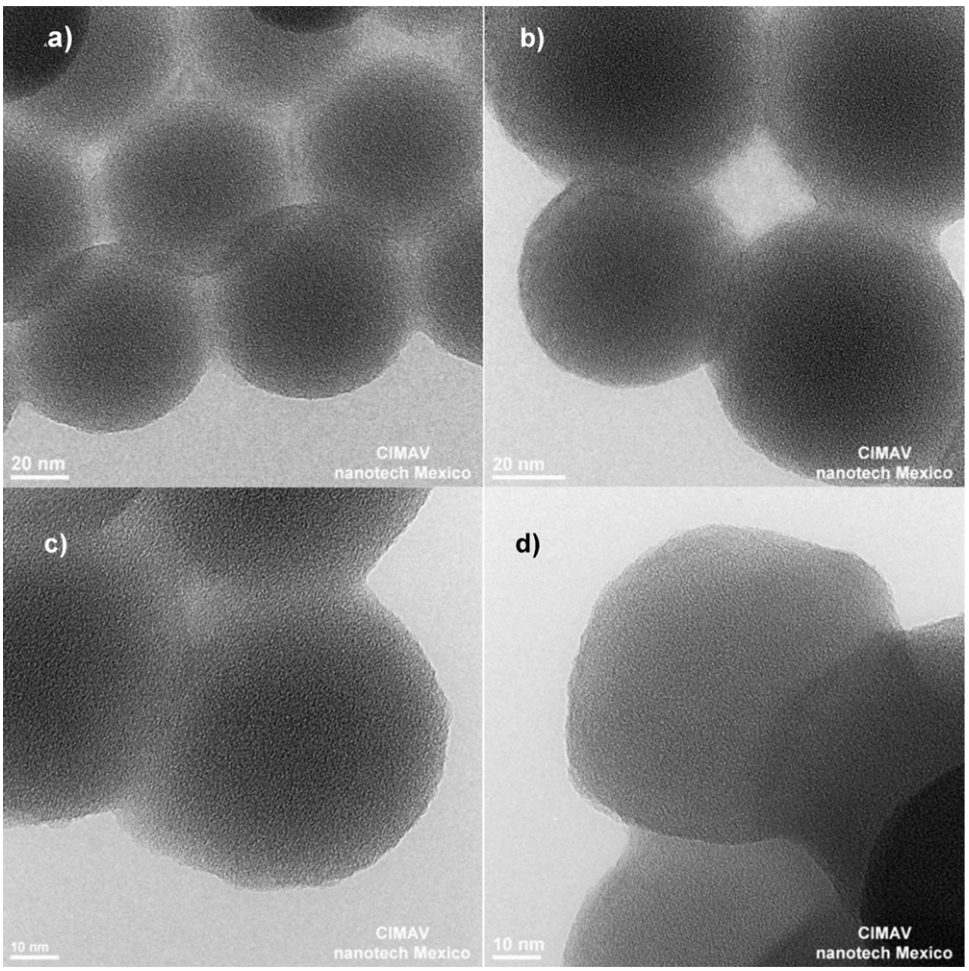

Fig. 8. Micrographs of HRTEM of the composites. (a) Pure polystyrene, (b) CPAni 3.3, (c) CPAni 18.7, and (d) CPAni 37.3.

3.5. Cyclic voltammetry

Cyclic voltammetric (CV) was used to determine PAni electroactivity. Fig. 6 shows voltammograms of core–shell composites recorded at sweep rate of 50 mV s^{-1}, in 0.5 M H_2SO_4 aqueous solution. In general, the composites exhibited two oxidation peaks and a reduction peak corresponding, respectively, to leucoemeraldine/emeraldine, and emeraldine/pernigraniline redox transitions [44]. The first oxidation peak, at 200 mV, was attributed to the oxidation of the fully reduced polyaniline (leucoemeraldine) to the radical cations (emeraldine salt) [45]. Whereas the second oxidation peak, at 640 mV, was attributed to the oxidation of the radical cations (emeraldine salt) to pernigraniline, accompanied by the exchange of protons, and vice versa for their corresponding reduction peaks [46]. In addition, the anodic peak, at 300 mV, represents the formation of benzoquinone (pernigraniline) [47].

The voltammetric behavior was similar to those obtained for substituted polyanilines [48,49]. The anodic and cathodic potential values corresponding to the first and second peaks, obtained from the voltammograms for different composites, are reported in Table 4. Hosseini and Entezami [50] reported the cyclic voltammograms of PAni/polystyrene blends, which presented two redox couples for oxidation potentials (425 mV, and 770 mV) and reduction (500 mV, and −150 mV).

3.6. Electrical conductivity

Electroconductivity of the composites and blank of polyaniline was determined by the 4-probe technique. The effect of PAni content on the electrical conductivity (σ) of the composites is illustrated in Fig. 7a. As observed, the composites and the pure PAni showed conductivity in the order of semiconductors (10^{-6} to 10^{-1} S cm^{-1}). Initially, with the increment of PAni, CPAni 3.3 to CPAni 26.7, conductivity increased linearly from 6.42×10^{-6} to 0.01 S cm^{-1}, whereas for CPAni 37.3, conductivity behavior changed. Such change has been observed for polymer/PAni systems at comparable PAni contents [51–53], where compatibility between PAni and the polymer host has been suggested to influence such behavior [54]. The so-called percolative conduction is the commonly accepted mechanism that describes electrical conduction of systems near metal-insulator transition containing conducting fillers. The principles of this mechanism have been introduced excellently by Kirkpatrick [55], Zallen [56], and Stauffer [57]. Percolation is described by $\sigma = k(V - V_f)^{\beta}$, where k is a constant, V and V_f stand, respectively, for volume fraction of the filler, and volume fraction of the filler at the percolation threshold. β is the critical exponent, which depends on the dimensionality of the space (1.0–1.6 for two-dimensional system, and 1.8–2.0 for three-dimensional system). The curve of Log σ versus Log $(V - V_f)$ is shown in Fig. 7b. Mathematical treatment gave values of k and β, of 2.8×10^{-8} and 3.96, respectively, and a theoretical V_f of 0.042% (0.059 wt%). Particularly, value of β was higher than the expected ($\beta = 2$, standard theory of percolation of transport universality). According to Grimaldi et al. [58,59] values of $\beta > 2$ may be described by the tunneling–percolation model, where tunneling processes between conducting particles, under some general circumstances (pressure or strain), could lead to transport exponents dependent of the mean tunneling distance.

3.7. Polyaniline shell

Result showed that all properties of the composites depended directly on PAni content. The study of the particle size distribution showed that PAni shell's contribution on the overall composite diameter was only slightly detectable at the highest PAni content (CPAni 37.3). Fig. 8(a)–(d) portraits micrographs of high resolution

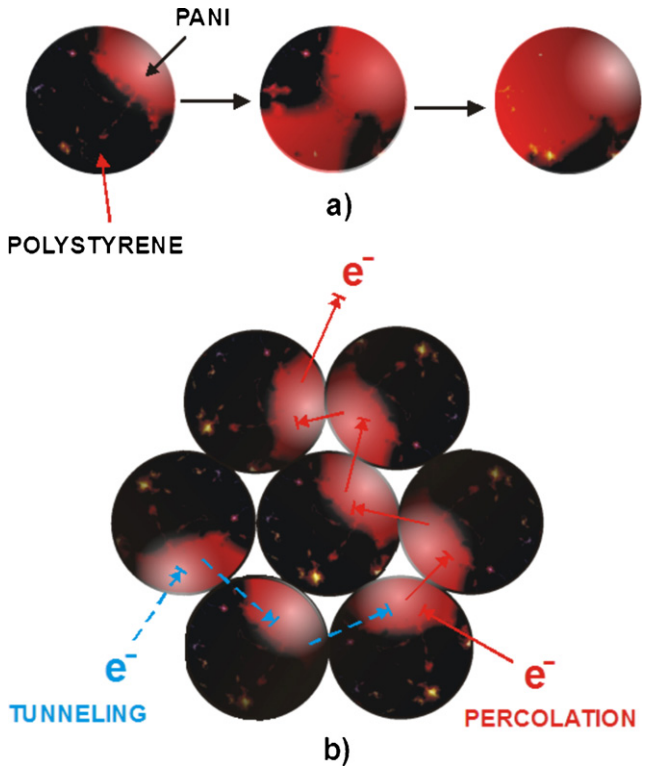

Fig. 9. (a) Model of PAni in the surface of composites, PAni concentration increases from left to right. (b) Tunneling–percolation conductivity on the surface of the core–shell composites.

(HR) TEM of pure polystyrene and the composites CPAni 3.3, CPAni 18.7, and CPAni 37.3. As observed, the particles show only progressive surface deformation, but no phase separation is perceivable. Consequently, PAni shells may be visualized as thin coatings instead of deposited aggregates (as mentioned before). We have calculated the ratio-grams of PAni shell/square meter of polystyrene core (see supplementary material Fig. S3). For CPAni 3.3, and CPAni 37.3 the ratios were, respectively, 0.0014 and 0.0216 g of PAni per m^2 of polystyrene. Evidently, these ratios are very low, which can explain the low impact of PAni content on the average particle diameter.

We consider that because of DS-AN surface properties (surfactant), it distributes homogeneously on the polystyrene cores surface. In this way, DS-AN polymerization is expected to occur over the polymer particles. Otherwise, agglomerations of PAni particles (polymerized in the aqueous phase) would be conforming the conducting shells; however, HRTEM showed no evidence of agglomeration of PAni particles but the formation of layers. Consequently, depending on the PAni content the core surface is more or less coated by a thin layer of the conducting material, as illustrated in Fig. 9(a). If a system with certain PAni content is considered, the arrangement in 2D illustrated in Fig. 9(b) can be assumed. For that, we must mention that samples for conductivity were prepared by manual compression and no thermal stress was applied. Consequently, the composite geometry settled during the synthesis is unaltered (spherical-solid particles). According to the figure, percolative conduction occurs over the surfaces in direct contact coated by PAni. However, when the polystyrene matrix allows it (thin enough region) tunneling conduction would be favored. Therefore, electrical conduction in the system occurs by the tunneling–percolation mixed mechanisms.

Under this scenario, besides of pressure and stress, as suggested by Grimaldi, temperature and interparticle free-volume are additional conditions that can modify conductivity, because of the thermoplastic nature of the core. Consequently, application of

mechanical stress, temperature, and stress-temperature are expected to affect electrical behavior. It is worth saying that because of the composite constitution, piezoresistivity may be exhibited since polystyrene properties are modified by the mentioned conditions. This study is under development, and is not considered here.

4. Conclusions

In summary, we successfully applied reactive surfactant DS-AN as the monomer of polyaniline to synthesize polystyrene/polyaniline core–shell composites via oxidative polymerization. Several analytical techniques gave evidence of polyaniline presence in the composites. According to electron microscopy, polyaniline was deposited on the polystyrene cores as a thin conducting layer, as shown by the low contribution of the polyaniline shells to the overall core–shell composite diameters, differently from several reports. From electroactive and electroconducting properties, we believe that it is possible to develop, based on the composites nature, materials with piezoresistive response for sensor design. This work led to a deeper understanding of DS-AN performance as a precursor of conducting-electroactive composite materials. In addition, thanks to its double function surfactant/monomer, the possibility of designing a variety of composite materials with different kinds of substrates; i.e., graphite for energy storage applications has been reveled.

Appendix A. Supplementary data

Supplementary data associated with this article can be found, in the online version, at http://dx.doi.org/10.1016/j.synthmet.2013.02.009.

References

[1] M.A. Khan, S.P. Armes, Advanced Materials 12 (2000) 671.
[2] M.M. Castillo-Ortega, T. Del Castillo-Castro, J.C. Encinas, M. Perez-Tello, M.A. De Paoli, R. Olayo, Journal of Applied Polymer Science 89 (2003) 179.
[3] C.H. Ho, C.D. Liu, C.H. Hsieh, K.H. Hsieh, S.N. Lee, Synthetic Metals 158 (2008) 630.
[4] V. Janaki, B.T. Oh, K. Shanthi, K.J. Lee, A.K. Ramasamy, S. Kamala-Kannan, Synthetic Metals 162 (2012) 974.
[5] C.S. Wu, eXPRESS Polymer Letters 6 (2012) 465.
[6] C. Barthet, S.P. Armes, M.M. Chehimi, C. Bilem, M. Omastova, Langmuir 14 (1998) 5032.
[7] L.Y. Yang, W.B. Liau, Materials Chemistry and Physics 115 (2009) 28.
[8] Q. Wu, Z. Wang, G. Xue, Advanced Functional Materials 17 (2007) 1784.
[9] Y. Li, Z. Wang, C. Wang, Z. Zhao, G. Xue, Polymer 52 (2011) 409.
[10] X.Y. Dai, X. Zhang, Y.F. Meng, P.K. Shen, New Carbon Materials 26 (2011) 389.
[11] P. Lacroix-Desmazes, A. Guyot, Macromolecules 29 (1996) 4508.
[12] S. Âbele, M. Sjöberg, T. Hamaide, A. Zicmanis, A. Guyot, Langmuir 13 (1997) 176.
[13] P. Reb, K.M. Margarit-Puri, M. Klapper, K. Müllen, Macromolecules 33 (2000) 7718.
[14] X. Wang, E.D. Sudol, M.S. El-Aasser, Langmuir 17 (2001) 6865.
[15] E.A. Zaragoza-Contreras, M. Stockton-Leal, C.A. Hernández-Escobar, Y. Hoshina, J.F. Guzmán-Lozano, T. Kobayashi, Journal of Colloid and Interface Science 377 (2012) 231.
[16] A. Guyot, Current Opinion in Colloid and Interface Science 1 (1996) 580.
[17] A. Guyot, C. Graillat, C. Favero, Comptes Rendus Chimie 6 (2003) 1319.
[18] A. Guyot, K. Tauer, Advances in Polymer Science 111 (1994) 43.
[19] J.M. Asua, H.A.S. Schoonbrood, Acta Polymerica 49 (1998) 671.
[20] A. Guyot, K. Tauer, J.M. Asua, S. Van Es, C. Gauthier, A.C. Hellgren, D.C. Sherrington, A. Montoya-Goni, M. Sjoberg, O. Sindt, F. Vidal, M. Unzue, H. Schoonbrood, E. Shipper, P. Lacroix-Desmazes, Acta Polymerica 50 (1999) 57.
[21] V.T. John, B. Simmons, G.L. McPherson, A. Bose, Current Opinion in Colloid and Interface Science 7 (2002) 288.
[22] N. Kuramoto, A. Tomita, Polymer 38 (1997) 3055.
[23] Y. Haba, E. Segal, M. Narkis, G.I. Titelman, A. Siegmann, Synthetic Metals 110 (2000) 189.
[24] V. Rumbau, J.A. Pomposo, J.A. Alduncin, H. Grande, D. Mecerreyes, E. Ochoteco, Enzyme and Microbial Technology 40 (2007) 1412.
[25] W. Yin, E. Ruckenstein, Synthetic Metals 108 (2000) 39.
[26] D. Tsotcheva, T. Tsanov, L. Terlemezyan, S. Vassilev, Journal of Thermal Analysis and Calorimetry 63 (2001) 133.
[27] L. Yu, J.I.I. Lee, K.W. Shin, C.E. Park, R. Holze, Journal of Applied Polymer Science 88 (2003) 1550.
[28] C. Basavaraja, R. Pierson, D.S. Huh, A. Venkataraman, S. Basavaraja, Macromolecular Research 17 (2009) 609.
[29] M. Okubo, S. Fugii, H. Minami, Colloid and Polymer Science 279 (2001) 139.
[30] M.S. Cho, Y.H. Cho, H.J. Choi, M.S. Jhon, Langmuir 19 (2003) 5875.
[31] E.C. Chen, Y.W. Lin, T.M. Wu, Polymer Degradation and Stability 94 (2009) 550.
[32] L. Sun, Y. Shi, L. Chu, X. Xu, J. Liu, Journal of Applied Polymer Science 126 (2012) 870.
[33] Y. Zhu, J. Zhang, Y. Zheng, Z. Huang, L. Feng, L. Jiang, Advanced Functional Materials 16 (2006) 568.
[34] Y. Fu, R.A. Weiss, Synthetic Metals 84 (1997) 103.
[35] H. Eisazadeh, A. Kavian, Polymer Composites 30 (2009) 43.
[36] N.V. Blinova, S. Reynaud, F. Roby, M. Trchová, J. Stejskal, Synthetic Metals 160 (2010) 1598.
[37] T.H. Hsieh, K.S. Ho, X. Bi, C.H. Huang, Y.Z. Wang, Y.K. Han, Z.L. Chen, C.H. Hsu, P.H. Li, Y.C. Chang, Synthetic Metals 160 (2010) 1609.
[38] E. Marie, R. Rothe, M. Antonietti, K. Landfester, Macromolecules 36 (2003) 3967.
[39] H. Hu, J.L. Cadenas, J.M. Saniger, P.K. Nair, Polymer International 45 (1998) 262.
[40] G. Ćirić-Marjanović, M. Trchová, J. Stejskal, Journal of Raman Spectroscopy 39 (2008) 1375.
[41] M.L. Boyer, S. Quillard, G. Louarn, G. Froyer, S. Lefrant, Journal of Physical Chemistry B 104 (2000) 8952.
[42] M. Trchová, I. Šeděnková, E. Tobolková, J. Stejskal, Polymer Degradation and Stability 86 (2004) 179.
[43] R. Ansari, M.B. Keivani, E-Journal of Chemistry 3 (2006) 202.
[44] G.M.O. Barra, R.R. Matins, K.A. Kafer, R. Paniago, C.T. Vasques, A.T.N. Pires, Polymer Testing 27 (2008) 886.
[45] D. Orata, D.A. Buttry, Journal of the American Chemical Society 109 (1987) 3574.
[46] S. Mu, Synthetic Metals 160 (2010) 1931.
[47] G. Li, S. Pang, H. Peng, Z. Wang, Z. Cui, Z. Zhang, Journal of Polymer Science Part A: Polymer Chemistry 43 (2005) 4012.
[48] H.K. Lin, S.A. Chen, Macromolecules 33 (2000) 8117.
[49] B.A. Deore, I. Yu, M.S. Freund, Journal of the American Chemical Society 126 (2004) 52.
[50] S.H. Hosseini, A.A. Entezami, Polymers for Advanced Technologies 12 (2001) 482.
[51] M. Sumita, K. Sakata, Y. Hayakawa, S. Asai, K. Miyasaka, M. Tanemura, Colloid and Polymer Science 270 (1992) 134.
[52] W.J. Bae, W.H. Jo, Y.H. Park, Synthetic Metals 132 (2003) 239.
[53] M.G. Han, J. Sperry, A. Gupta, C.F. Huebner, S.T. Ingramb, S.H. Foulger, Journal of Materials Chemistry 17 (2007) 1347.
[54] S.H. Kim, K.W. Oh, T.K. Kim, Journal of Applied Polymer Science 96 (2005) 1035.
[55] S. Kirkpatrick, Reviews of Modern Physics 45 (1973) 574.
[56] R. Zallen, The Physics of Amorphous Solids, John Wiley & Sons, New York, 1983, pp. 135–191.
[57] D. Stauffer, A. Aharony, Introduction to Percolation Theory, Taylor & Francis, London, 1985.
[58] S. Vionnet-Menot, C. Grimaldi, T. Maeder, S. Strässler, P. Ryser, Physical Review B 71 (2005) 064201.
[59] C. Grimaldi, I. Balberg, Physical Review Letters 96 (2006) 066602.